https://doi.org/10.15407/ujpe71.7.586

O.D. STOLIARYK,[1] O.V. KHOROLSKYI[2]

[1] Odesa I.I. Mechnikov National University
(2, V. Zmiienka Str., Odesa 65026, Ukraine; e-mail: adiabata384@gmail.com)
[2] Poltava V.G. Korolenko National Pedagogical University
(2, Ostrograds'kogo Str., Poltava 36000, Ukraine; e-mail: khorolskiy.alexey@gmail.com)

THE SPECIFICITY OF HYDROGEN BONDS IN WATER

A specific manifestation of hydrogen bonding in the structural and thermodynamic properties of liquid water has been analyzed. Based on a particular molecular structure of water, a novel mechanism for water dimer formation and the concurrent emergence of hydrogen bonding has been proposed. It was found that the characteristic angles of a water dimer are in good agreement with experimental data. It was demonstrated that the discrepancy between the coexistence curves of water and argon is caused by short-range hydrogen bonds available within the whole interval of water existence in the liquid state. It has been proven that the absence of long-range hydrogen bonds in water is associated with the instability of their transverse thermal excitations. Characteristic temperature values for liquid water were examined.

K e y w o r d s: water, hydrogen bonds, thermodynamic properties, kinetic properties.

1. Introduction

Ice melting is accompanied by the breaking of hydrogen bonds; otherwise, it would be impossible to reconcile the experimentally observed values of the kinematic shear viscosity of water with the values characteristic of other low-molecular-weight liquids without hydrogen bonds. Thus, at a temperature of $1.2T_{\rm tr}^{\rm (w)}$, where $T_{\rm tr}^{\rm (w)} = 273.16$ K is the triple point temperature of water, the kinematic shear viscosity of water equals $\nu_{\rm w}(328\ {\rm K}) = 0.5 \times 10^{-2}$ cm^2/s [1, 2], whereas for argon at a temperature of $1.2T_{\rm tr}^{\rm (Ar)}$, where $T_{\rm tr}^{\rm (Ar)} = 83.81$ K is the triple point temperature of argon, its kinematic shear viscosity equals $\nu_{\rm Ar}(100\ {\rm K}) = 0.12 \times 10^{-2}$ cm^2/s [3]. That is, their kinematic shear viscosities are of the same order of magnitude, which would be impossible if most water molecules were connected to one another by hydrogen bonds.

In order to understand the reasons for such behavior of the shear viscosities of water and argon, we will

1) use the hydrogen bonding model described in works [4, 5] and

2) use intermolecular potentials of the Simple Point Charge (SPC) type in calculations; the SPC model is one of the most common models of the water molecule, in which the molecule is considered as a rigid three-center system with point charges located at the hydrogen and oxygen atoms [6].

Thus, we assume that the water molecule is built on the basis of a cubic framework. The oxygen ion O^{2-} is located at the geometric center of the cell, two hydrogen atoms occupy diametrically opposite vertices of the upper cube face, and effective negative charges are located at diametrically opposite vertices of the lower cube face, as described in Ref. [4]. The electron shell of the oxygen ion, which favors the formation of the spatial structure of the water molecule, arises due to four outer electrons, which become "stretched" along the cube diagonals, as is shown in Fig. 1. Such a configuration of the electron shell minimizes the energy of the electric field formed by the O^{2-} ion. The formation of a hydrogen bond when two water molecules oriented according to the dimer configuration approach each other is demonstrated in Figs 1 and 2.

The interaction energy between two molecules oriented in the dimer configuration depends on the dis-

Citation: Stoliaryk O.D., Khorolskyi O.V. The specificity of hydrogen bonds in water. *Ukr. J. Phys.* **71**, No. 7, 586 (2026). https://doi.org/10.15407/ujpe71.7.586.

tance $r_{O_1O_2}$ between the oxygen atoms (see Fig. 2) as follows:

1) if $r_{O_1O_2} > 2l_H$, where l_H is the hydrogen bond length, then the interaction energy is determined primarily by the Coulomb interaction between the effective positive and negative charges;

2) in the opposite case, $r_{O_1O_2} < 2l_H$, the electron shells of both molecules cover the hydrogen, i.e., a standard hydrogen bond is formed (Fig. 2, *b*).

The length and energy of hydrogen bonds substantially depend on their formation conditions. If the hydrogen bond corresponds to an isolated dimer, then $l_H^{(D)} = 2.96$ Å (see Table 1). The hydrogen bond length in hexagonal ice is somewhat smaller, $l_H^{(I)} = 2.76$ Å. However, in water, it is believed that $l_H^{(w)} = 2.04$ Å. Such behavior of hydrogen bonds is determined by the influence of strong electric fields of neighboring molecules, as well as screening effects.

In this work, we will consider the following problems: 1) the parameters of dimers formed in water; 2) the features of the thermal motion of water molecules in a wide range of its existence from the triple point to the critical point; we will consider the emergence of characteristic temperature values; 3) conditions for the formation of hydrogen bonds in liquid water; 4) longitudinal and transverse vibrations of the hydrogen bond in the dimer; and 5) mechanisms of hydrogen bond destruction.

The scientific novelty of the work lies in the study of the specific features of the manifestation of hydrogen bonds in the structural and thermodynamic properties of liquid water. The structure of the work is determined by the following logic. The goal and tasks of the work are formulated in the Introduction. In Section 2, the main properties of hydrogen bonds are considered. In Section 3, the spatial structure of the water dimer is analyzed, which allows us to establish, in Section 4, the prerequisites for the formation of hydrogen bonds. In Section 5, on the basis of the temperature dependence of the residence time and dipole relaxation, the values of the characteristic water temperatures are obtained, the coexistence curves of water and argon are compared, and a conclusion is drawn about the short-term existence of hydrogen bonds within the entire range of water existence in the liquid state. Section 6 is devoted to an analysis of transverse and longitudinal vibrations of the hydrogen bond, which can confirm the hypothesis about the absence of long-term hydrogen bonds in water, which is further discussed in Section 7.

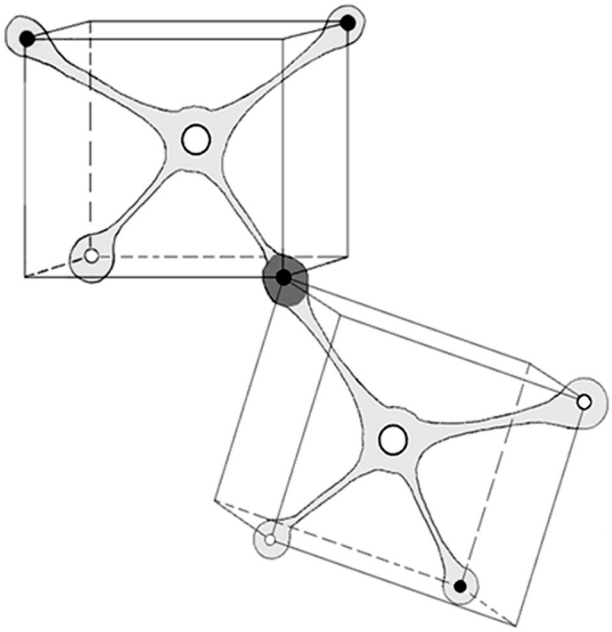

Fig. 1. Structure of the dimer $(H_2O)_2$ according to Ref. [4]. The following notations are used: (•) hydrogens in water molecules; (◯) oxygens, (∘) effective negative charges that arise due to the specificity of the electron shells of oxygen atoms

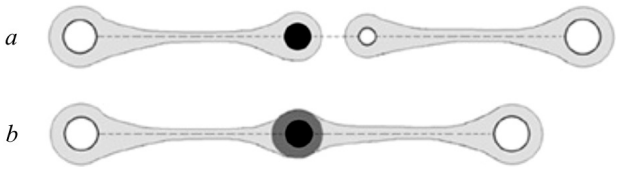

Fig. 2. Model of a hydrogen bond described in Ref. [4]. Charge distributions: before the extended electron shell of the right molecule covered the hydrogen atom in the left molecule, $r_{O_1O_2} > 2l_H$ (*a*); and after the overlap occurred, $r_{O_1O_2} < 2l_H$(*b*). Here, l_H is the hydrogen bond length

2. Basic Properties of Hydrogen Bonds

The basic properties of hydrogen bonds in water include their energy ε_H and length l_H, as well as the lifetime τ_H. Note that the interaction energy will be described in units of the thermal noise energy k_BT_{tr}, where T_{tr} is the triple point temperature, and the lifetime of hydrogen bonds in units of the time of a complete molecular rotation, $\tau_0 = 2\pi/\omega_r$, where $\omega_r = \sqrt{k_BT_{tr}/I_r}$ is the cyclic frequency of rota-

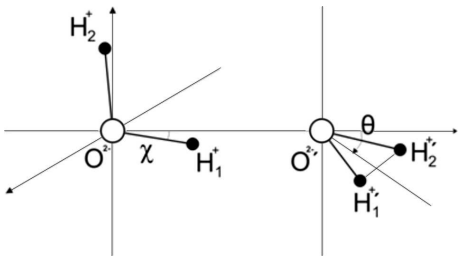

Fig. 3. Schematic diagram of a water dimer [18]

tional motion, and $I_r = 2m_{\mathrm{H}} r_{\mathrm{OH}}^2 \sin^2(\alpha/2)$ is the moment of inertia of the water molecule. Assuming that $\alpha = 104.5°$, $m_{\mathrm{H}} = 1.66 \times 10^{-24}$ g, and $r_{\mathrm{OH}} = 0.96 \times 10^{-8}$ cm, we find that $\tau_0 \approx 0.5 \times 10^{-12}$ s [7]. These values were determined by various methods and are listed in Table 1. The first column contains the designations of the most common potentials of intermolecular interaction in water: B stands for the Bernal potential, as a model of the interaction between water molecules [8]; BC stands for the Bernal–Carrington potential, a modification of the Bernal model with a refined description of intermolecular interaction [9]; SPC (Simple Point Charge) stands for the model of a water molecule with three point charges located at the hydrogen and oxygen atoms [6]; SPC/E (Extended Simple Point Charge) stands for the modified SPC model, which takes into account a correction for the polarization energy [10]; TIPS (Transferable Intermolecular Potential) stands for the transferable intermolecular potential parameterized to describe the properties of water over a wide range of conditions [11]; and TIP3P (Transferable Intermolecular Potential with 3 Points) stands for the three-center model of a water molecule, where the charges are located at three atoms of the molecule [12]. The corresponding values of ε_{H} and l_{H} were calculated in Refs. [11, 12]. In addition, Table 1 shows the values of the indicated hydrogen bond parameters obtained for water dimers (Dimer base) by microwave spectroscopy [13], for ice (Ice base) and liquid water (Liquid water) by X-ray Raman spectroscopy [14], and at temperatures of 280 and 310 K by the molecular dynamics (MD) method [15–17].

Table 1. **Values of the parameters ε_{H}, l_{H}, and τ_{H}**

Method and source	$l_{\mathrm{H}} \times 10^8$, cm	$\varepsilon_{\mathrm{H}}/k_{\mathrm{B}}T_{\mathrm{tr}}$	τ_{H}/τ_0
B [8]	2.96	–8.5	
BC [9]	2.89	–9.65	
SPC [6]	2.72	–12.49	
SPC/E [10]	2.72	–12.49	
TIPS [11]	2.7	–12.66	
TIP3P [12]	2.69	–12.90	
Dimer base [13]	2.976		
Ice base [14]	2.76	–12.38	
Liquid water [14]	2.81	–13.27	2
MD (280 K) [15–17]		–10.08	27
MD (310 K) [15–17]		–9.76	15

Furthermore, in the dimer model of hydrogen bonding, its energy is considered equal to

$$\varepsilon_{\mathrm{H}} = \Phi(r_{\mathrm{d}}, \Omega_{\mathrm{d}}), \quad l_{\mathrm{H}} = r_{\mathrm{d}}, \tag{1}$$

where $\Phi(r_{\mathrm{d}}, \Omega_{\mathrm{d}})$ is the interaction energy of water molecules in the equilibrium configuration of the dimer, $r_{\mathrm{d}} = r_{\mathrm{O_1O_2}}$, Ω_d is a set of equilibrium angles that determine the spatial structure of the dimer.

The intermolecular interaction potential was modeled as the sum of several independent contributions:

$$\Phi(r, \Omega) = \Phi_r(r, \Omega) + \Phi_{\mathrm{D}}(r, \Omega) + \\ + \Phi_{\mathrm{el}}(r, \Omega) + \Phi_{\mathrm{H}}(r, \Omega), \tag{2}$$

where $\Phi_r(r, \Omega)$ is the repulsive component, $\Phi_{\mathrm{D}}(r, \Omega)$ is the dispersion interaction component, $\Phi_{\mathrm{el}}(r, \Omega)$ is the electrostatic interaction energy between two water molecules, and $\Phi_{\mathrm{H}}(r, \Omega)$ is the irreducible hydrogen bond interaction energy [1, 2].

3. Dimer as the Simplest Manifestation of Hydrogen Bonding

If we retain only the images of the centers of mass of the hydrogen and oxygen ions in water molecules in Fig. 1, then the water dimer takes the form presented in Fig. 3. The ions in Fig. 3 are depicted as centers of mass without taking into account their van der Waals sizes, so the figure does not exhibit the real diameter of the water molecule.

To determine the parameters of the dimer, we will proceed from the model shown in Fig. 3, where the dimer can be considered as a combination of a hydroxonium ion (see Fig. 4, *a*) and a hydroxyl ion (see Fig. 4, *b*). The unit vectors directed toward the vertices of the cube, in which the water molecules are located, are determined by the relationships

$$\mathbf{e}_{OA} = \frac{1}{\sqrt{3}} (\mathbf{i} + \mathbf{j} - \mathbf{k}), \tag{3}$$

$$\mathbf{e}_{OB} = \frac{1}{\sqrt{3}}(\mathbf{i} - \mathbf{j} + \mathbf{k}), \tag{4}$$

$$\mathbf{e}_{OC} = \frac{1}{\sqrt{3}}(-\mathbf{i} + \mathbf{j} + \mathbf{k}). \tag{5}$$

The valence angle, i.e., the angle between the lines connecting the oxygen atom and the hydrogen atoms, is determined by the equation

$$\angle(\mathrm{HOH}) = \arccos(\mathbf{e}_{OA} \cdot \mathbf{e}_{OB}) = \\ = \arccos(-1/3) = 109.5^\circ. \tag{6}$$

This angle is approximately 4° larger than the bond angle in an isolated water molecule. The angle θ in Fig. 3 is equal to the angle between the directions formed by the z-axis and the unit vector $\mathbf{e}_{OA}$,

$$\theta = \arccos(\mathbf{k} \cdot \mathbf{e}_{OA}) = \arccos(1/\sqrt{3}) \approx 52^\circ. \tag{7}$$

The experimental values of this angle are given in Table 2.

As can be seen, the obtained value of the angle θ agrees quite satisfactorily with the experimental data. The discrepancies in the θ-values in Refs. [19–21] arise from differences in the molecular dynamics simulation methodologies: the non-pair additive potential method, implemented by introducing the polarizability into the model [19], the method of self-consistent field of molecular orbitals, implemented from first principles without empirical parameters (*ab initio* SCF-MO) [20], and the method implemented at the level of second-order Möller–Plesset perturbation theory (MP2) [21].

In addition, the length of the cube side for an isolated water molecule equals

$$a = \frac{2}{\sqrt{3}} r_{OA} \approx 1.109 \text{ Å}, \tag{8}$$

and, according to Fig. 1, the length of the hydrogen bond is

$$l_{\mathrm{H}} \approx 2r_{OA} \approx 2 \text{ Å}, \tag{9}$$

which also agrees quite satisfactorily with the experimental data for water (see Table 1).

4. Preliminary Condition for Hydrogen Bond Formation

In order to better understand the origins of the behavior of the settling time $\tau_0(t)$ and the dipole relaxation time $\tau_{\mathrm{d}}(t)$, where $t = T/T_c$ is the relative temperature normalized to the critical temperature of water, let us consider the ratio between the average hydrogen bond length in ice, $l_{\mathrm{H}}^{(\mathrm{I})} = 2.67$ Å, and the average distance between molecules in liquid water, $a = n^{-1/3}$. If the dimensionless parameter $\zeta_{\mathrm{I}}(t) = l_{\mathrm{H}}^{(\mathrm{I})} n^{1/3}(t) \ll 1$, then the formation of stable hydrogen bonds between neighboring molecules is impossible. Hydrogen bonds with the length $l_{\mathrm{H}}^{(\mathrm{w})} = 2.04$ Å also arise in water; they correspond to the dimensionless parameter $\zeta_{\mathrm{w}}(t) = l_{\mathrm{H}}^{(\mathrm{w})} n^{1/3}(t)$. As a result of the hydrogen bond formation, dimers and higher-order multimers with short lifetimes may arise. This parameter increases significantly when approaching the critical point due to a significant expansion of the system [22, 23] and the increase in the volume per dimer, first of all.

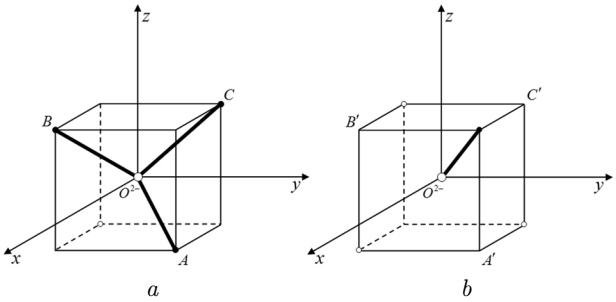

Fig. 4. Models of hydroxonium ion $(H_2O)H^+$ (*a*) and hydroxyl (*b*) in a Cartesian coordinate system. The following notations are used here: (•) hydrogens, (◯) oxygens, (∘) effective negative charges that arise due to the specificity of the electron shells of oxygen atoms

The behavior of $\zeta_{\mathrm{d}}(t)$, $\zeta_{\mathrm{I}}(t)$, and $\zeta_{\mathrm{w}}(t)$ along the vapor-liquid coexistence curve is presented in Fig. 5. As can be seen, these parameters vary within the following limits:

$$0.65 < \zeta_{\mathrm{d}}(t) < 0.96, \tag{10}$$

$$0.61 < \zeta_{\mathrm{I}}(t) < 0.9, \tag{11}$$

$$0.61 < \zeta_{\mathrm{w}}(t) < 0.9, \tag{12}$$

where the lower limit corresponds to the vicinity of the critical point, and the upper limit to the triple point.

Table 2. **Values of the angle θ in the equilibrium state**

Source	[19]	[20]	[21]
Angle θ, deg.	51.8	60	57 ± 10

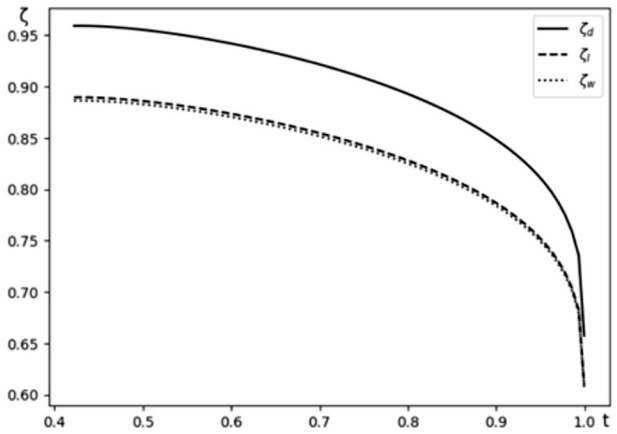

Fig. 5. Dependences of the quantities $\zeta_{\rm d}$, $\zeta_{\rm I}$, and $\zeta_{\rm w}$ on the relative temperature $t = T/T_c$

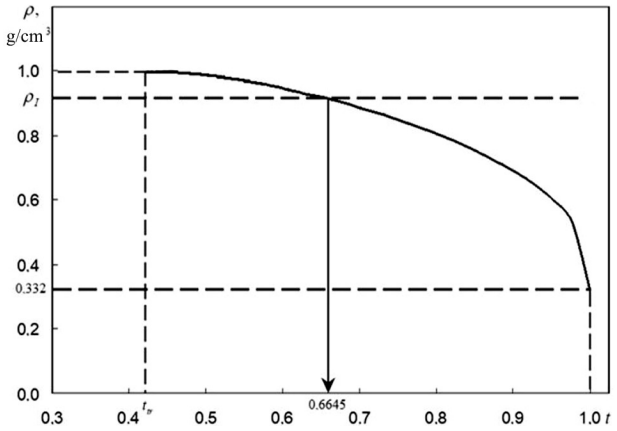

Fig. 6. Comparison of the temperature dependences of the water and ice densities near the triple point temperature

Inequalities (10)–(12) indicate that in the existence interval of liquid water, the formation of a stable hydrogen-bond network is impossible. Hydrogen bonds arise only as a result of a random approach of neighboring molecules to the distance $r_{12} \approx l_{\rm H}$. Similarly, water dimers can arise, as well as tetramers and more complex clusters.

4.1. Characteristic temperatures of water

The melting of hexagonal ice is accompanied by the destruction of the hydrogen bond network and a change in the system density. Within a short temperature interval, the density of water increases insignificantly and then, up to the critical point, decreases according to a law close to an argon-like one (see Fig. 6).

It is clear that the temperature $T_{\rm w}$ determined by the equation

$$\rho_{\rm I}(T_{\rm tr}) = \rho_{\rm w}(T_{\rm w}) \tag{13}$$

allows us to estimate the temperature interval $T_{\rm w} - T_{\rm tr}$ within which multiparticle correlations vanish. From Fig. 6, it follows that

$$T_{\rm w} = 0.6645\, T_c \approx 430 \text{ K}. \tag{14}$$

A surprising result is obtained if the density of water between the triple and critical points is approximated by a linear dependence on temperature,

$$\rho_{\rm w}(t) = \rho_{\rm w}(t_{\rm tr}) + \frac{t - t_{\rm tr}}{1 - t_{\rm tr}} \left[\rho_{\rm w}(1) - \rho_{\rm w}(t_{\rm tr})\right]. \tag{15}$$

In this case, the equation $\rho_{\rm w}(t_L) = \rho_h(t_{\rm tr})$, similar to Eq. (13), yields the temperature: $t_L \approx 0.485$, which coincides with the upper limit of the crystal-like motion of molecules in water ($T_{\rm H} \approx 315$ K). However, this approach to determining $T_{\rm H}$ is unrelated to the features of the thermal motion of molecules.

It is clear that Eq. (13) can also be rewritten in the form $n_{\rm w}(t_{\rm H}) = n_h(t_{\rm tr})$, where n denotes the concentration of water or ice molecules, as well as in the form $\zeta_{\rm w}(t_{\rm H}) = \zeta_h(t_{\rm tr})$.

5. Properties of the Hydrogen Bond Network in Liquid Water

In this section, we will analyze the properties of a random hydrogen bond network formed in liquid water.

5.1. Macroscopic manifestations of hydrogen bonds in water

The character of the thermal motion of molecules in water is determined by the features in the translational and rotational motion of its molecules. Important characteristics of the former are the settling time τ_0 and the transition time τ_f between temporary vibrational positions of the molecule. With satisfactory accuracy, the time τ_f can be approximated by the expression: $\tau_f \sim a/v_r$, where a is the average interparticle distance, and v_r is the average velocity of thermal motion. The temperature dependence of the ratio $\tilde{\tau}_0 = \tau_0/\tau_f$ was obtained in Refs. [24, 25] on the basis of data on quasi-elastic incoherent scattering of slow neutrons and is shown in Fig. 7.

An analysis of dipole relaxation provides important information about the rotational motion of water molecules. The most important quantity here is the ratio between the dipole relaxation time $\tau_{\rm d}$ and the period of thermal rotation of a free molecule, $\tau_r \sim 2\pi/\omega_T$, where $\omega_T \sim \sqrt{k_{\rm B}T/I}$ is the characteristic angular velocity, $I \sim m_{\rm H} r_{\rm OH}^2$ is the moment of inertia of the water molecule ($m_{\rm H}$ is the mass of the hydrogen atom, and $r_{\rm OH}$ is the distance between the hydrogen atoms and the oxygen atom). With satisfactory accuracy, we find that $\tau_r \approx 5 \times 10^{-13}$ s. The temperature dependence of the ratio $\tilde{\tau}_{\rm d} = \tau_{\rm d}/\tau_r$, according to several sources, was plotted in Ref. [27] and is shown in Fig. 8.

As can be seen, substantial deviations of $\tilde{\tau}_0$ and $\tilde{\tau}_{\rm d}(t)$ from unity are observed at $t < 0.5$. It is in this temperature range that the behavior of $\tilde{\tau}_{\rm d}(t)$ can be approximated by an exponential function (the dashed curve in Fig. 8)

$$\tilde{\tau}_{\rm d} = \tilde{\tau}_{\rm d}^{(0)} \exp(\varepsilon_{\rm H}/t), \tag{16}$$

where $\varepsilon_{\rm H} = E_{\rm H}/(k_{\rm B}T_{\rm tr})$, $\tilde{\tau}_{\rm d}^{(0)} = 5.1 \times 10^{-4}$, and $\varepsilon_{\rm H} = 11.2$. It is important that the value of the activation energy $\varepsilon_{\rm H}$ practically coincides with the hydrogen bond energy for most of the model potentials listed in Table 1. During the settled lifetime $\tau_0 \sim \tau_{\rm d}$, the dipole moment of the water molecule oscillates around the direction imposed by the external alternating field, and afterward the ordering of the dipole-moment orientations is lost. The deviation of the dashed curve from the experimental values of the dipole relaxation time occurs near $t_{\rm d} \approx 0.48 \div 0.49$, which corresponds to the upper limit of the crystal-like vibrations of water molecules determined from the analysis of translational motion.

Thus, the analysis of translational and rotational motions leads to the self-consistent conclusion that the crystal-like character of the motion of liquid water molecules occurs within the temperature interval

$$T_{\rm tr} = 273 \text{ K} < T < T_{\rm H} \approx 315 \text{ K}. \tag{17}$$

At the same time, the behaviors of $\tilde{\tau}_0(t)$ and $\tilde{\tau}_{\rm d}(t)$ at higher temperatures, although remaining close to unity, differ substantially. The values of $\tilde{\tau}_0$ approach unity and become even smaller, whereas the values of $\tilde{\tau}_{\rm d}(t)$ are 2 to 3 times larger than unity in the temperature interval $0.48 < t < 1$ and approach it very slowly.

5.2. Optimal fitting of the water coexistence curve to the argon one

In Refs. [31, 32], it was found that the water coexistence curve $\tilde{v}_{\rm w}(t) = v_{\rm w}(t)/v_{\rm w}^{(c)}$ and the argon coexistence curve $\tilde{v}_{\rm Ar}(t) = v_{\rm Ar}(t)/v_{\rm Ar}^{(c)}$, both normalized to the corresponding critical values of the specific volumes, do not coincide, but up to $t \approx 0.9$, they exhibit similar behavior. They look like quasi-parallel curves shifted with respect to each other by a factor of 1.54. The character of their behavior changes significantly only in the vicinity of the Ginzburg temperature $t_{\rm G} = 0.97$. Upon approaching it, the water and argon coexistence curves intersect and lose their similar behavior.

In order to optimally fit the water coexistence curve to the argon one, let us consider the temperature de-

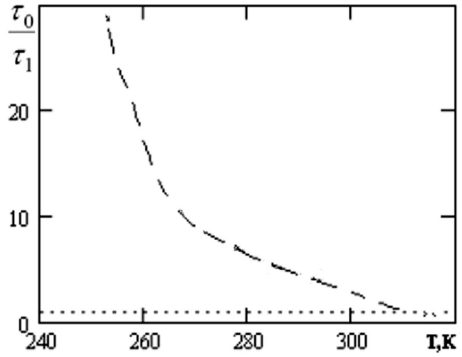

Fig. 7. Temperature dependence of the ratio τ_0/τ_f (the transition time is practically independent of temperature and is close to $\tau_f \approx 5 \times 10^{-13}$ s)

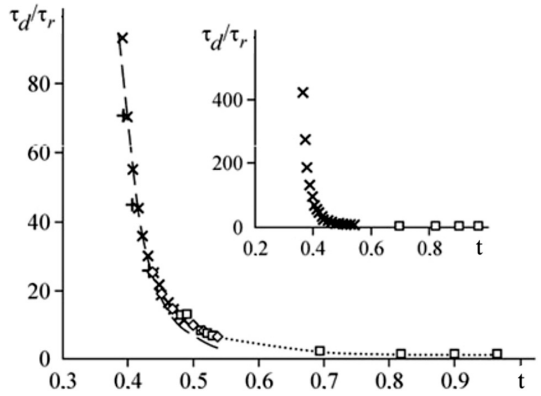

Fig. 8. Temperature dependence for the ratio $\tau_d(t)/\tau_r$, where τ_d was taken from Refs. [28] (+), [29] (□, ×), and [30] (◇). The extrapolated values of $\tau_d(t)$ are shown by dots. $t = T/T_c$

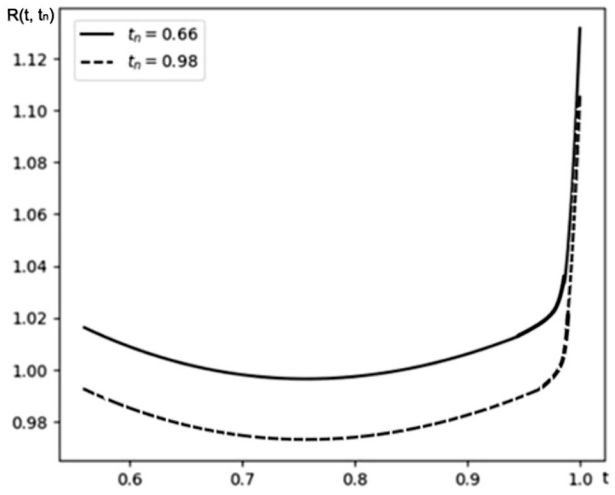

Fig. 9. Behavior of the function $R(t, t_n)$ for water and argon at the normalized temperatures $t_n = 0.66$ (solid curve) and 0.98 (dashed curve)

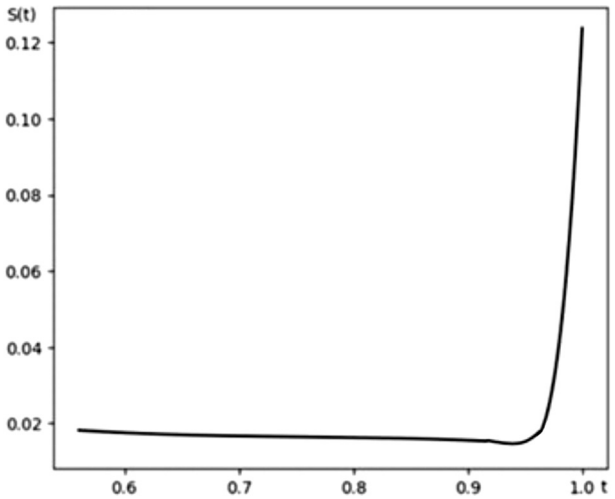

Fig. 10. Dependence of $S(t_n)$

pendence of the function

$$R(t, t_n) = \lambda_n \frac{v_{\rm w}(t)}{v_{\rm Ar}(t)}, \tag{18}$$

where

$$\lambda_n = \frac{v_{\rm Ar}(t_n)}{v_{\rm w}(t_n)},$$

$t = T/T_c^{(\rm w)}$ for water, and $t = T/T_c^{(\rm Ar)}$ for argon, as it should be. At the point $t = t_n$, the ratio $R(t, t_n) = 1$, slightly deviating from unity on the left- and right-hand sides, but increasing noticeably in the vicinity of the critical point, $t_{\rm G} < t < 1$. The behavior of the ratio $R(t, t_n)$ for the values $t_{n_1} = 0.66$ and $t_{n_2} = 0.98$ is shown in Fig. 9.

These curves appear almost identical, although being shifted parallel to each other, and provide no advantage in choosing the fractional volume with respect to which the normalization is performed. In this regard, let us define the function

$$S(t_n) = \sum_{1 \leqslant i \leqslant 440} \left[R(t_i, t_n) - 1\right]^2, \tag{19}$$

which describes the root-mean-square deviation of the water coexistence curve from the argon coexistence curve, provided that $t_i = 0.56 + 0.001\, i$. Let the values of t_n run through the same t_i-values. The character of the dependence $S(t_n)$ is presented in Fig. 10. One can see that the smallest relative deviation between the water and argon coexistence curves is observed at t_n =0.975; at this point, $\lambda_n = v_{\rm Ar}(t_n)/v_{\rm w}(t_n)|_{t_n=0.975} = 1.000$, i.e., the indicated curves intersect or touch each other.

Furthermore, at the first stage of the calculation, in the ratio $v_{\rm w}(t)/v_{\rm Ar}(t)$, which is obtained on the basis of experimental data for fractional volumes, each term is approximated by eleventh-order polynomials. As a result, $v_{\rm w}(t)/v_{\rm Ar}(t) = P_{11}^{(\rm w)}(t)/P_{11}^{(\rm Ar)}(t)$. In what follows, only polynomial approximations were used at each step. The behavior of $S(t_n)$ depending on the choice of the normalization point t_n is shown in Fig. 10.

As follows from Fig. 10, the function $S(t_n)$

1) demonstrates that the deviation of the ratio $R(t, t_n)$ from unity is less than 3%, namely,

$$R(t, t_n) \leqslant 1 \pm \sqrt{S(t_n)} \approx 1 \pm 0.1,$$

within almost the entire interval of liquid argon existence;

2) the minimum deviation of the ratio $R(t, t_n)$ from unity is observed at $t_n \approx 0.97$, which numerically coincides with the Ginzburg temperature.

In the zeroth approximation, the coexistence curves of water and argon should coincide, since they are described by the same interaction potentials, which are of the Lennard-Jones form. A small deviation of the water coexistence curve from the argon-like dependence is caused by the influence of hydrogen bonds, and from Fig. 10 it follows that their manifestation

is observed within the whole interval of water existence, including the critical point. As the temperature increases, the influence of hydrogen bonds gradually decreases, but does not vanish completely.

This conclusion

1) is fully consistent with the analysis of the behavior of the dielectric permittivity (see the next subsection), according to which, close to the temperature $T_\varepsilon \approx 0.85T_c$, a cluster structure is preserved in water, which owes its origin to short-term hydrogen bonds;

2) raises the issue of the need for a thorough experimental study of the temperature dependence of the ratio between the dipole relaxation time and the free rotation time of a water molecule, $\tilde{\tau}_\mathrm{d} = \tau_\mathrm{d}/\tau_r$.

5.3. Thermal excitations of clusters

In order to better understand the character of the thermal motion of water molecules at temperatures $0.48 < t < 1$, let us recall the conclusions drawn in Ref. [33] after analyzing the behavior of the dielectric permittivity. According to Refs. [7, 33], in the temperature range $0.42 < t < 0.85$, the polarization properties of water are formed by thermal vibrational excitations of water clusters, mainly tetramers. In this case, $\tau_\mathrm{d}(t)$ can be interpreted as the lifetime of tetramers, and the inequality $\tilde{\tau}_\mathrm{d}(t) > 1$ is naturally explained. As the temperature approaches $t \sim 0.48$, the tetramers combine into larger clusters, and the translational motion of the molecules acquires a vibrational character. Here, the unifying element is hydrogen bonds. As the temperature increases away from $t \sim 0.48$ toward higher temperatures, the vibrations of water molecules disappear, and their translational motion resembles the motion of atoms in argon. In the latter, the continuous chaotic drift of molecules is a consequence of the fact that the energy of thermal motion of molecules is comparable to the depth of the potential energy of interaction between the nearest neighbors, $k_\mathrm{B}T \approx 120$ K [2].

6. Longitudinal and Transverse Vibrations of Hydrogen Bond

The potential of intermolecular interaction in a water dimer can be approximated by the following averaged potential, which has the Lennard-Jones form:

$$U(r) = 4\varepsilon\left[\left(\frac{\sigma}{r}\right)^{12} - \left(\frac{\sigma}{r}\right)^{6}\right], \tag{20}$$

where the dimensional parameters obtained using the SPC/E potential are

$$\varepsilon \approx 2k_\mathrm{B}T_\mathrm{tr}, \quad \sigma \approx 2.7 \text{ Å}. \tag{21}$$

In the vicinity of the potential minimum $U(r_0) = -\varepsilon$, which takes place at $r_0 = 2^{1/6}\sigma$, the potential can be described by the series expansion

$$U(r) = -\varepsilon + \frac{36\varepsilon}{2^{1/3}\sigma^2}(r - r_0)^2 + \dots . \tag{22}$$

As a result, the elastic constant equals

$$k_{rr} = \left.\frac{\partial^2 U(r)}{\partial r^2}\right|_{r=r_0} = \frac{72\varepsilon}{2^{1/3}\sigma^2}. \tag{23}$$

The root-mean-square value of the longitudinal fluctuations of the hydrogen bond length is

$$\left\langle(\Delta r)^2\right\rangle = \frac{2^{1/3}k_\mathrm{B}T_\mathrm{tr}}{72\varepsilon}\sigma^2 t \tag{24}$$

or

$$\sqrt{\frac{\left\langle(\Delta r)^2\right\rangle}{\sigma^2}} \approx 0.1t. \tag{25}$$

Since the gap between the nearest neighbors in water also has a value of about 0.1σ [18], we see that its value is of the same order of magnitude as the longitudinal fluctuations of the hydrogen bond length.

Note that formula (20) can actually be written on the basis of dimensional considerations.

The interaction potential of water molecules in an isolated dimer as a function of the distance between oxygens is presented in Fig. 11, which is taken from Ref. [18].

The elastic constant of longitudinal vibrations is determined by the relationship

$$k_{rr} = \left.\frac{\partial^2 \Phi(r, \Omega_\mathrm{d})}{\partial r^2}\right|_{r=r_\mathrm{d}}, \tag{26}$$

and, according to Fig. 11, we obtain

$$k_{rr} = 4.23 \times 10^{17} k_\mathrm{B}T_\mathrm{tr} \text{ cm}^{-2}. \tag{27}$$

Let us compare this value with the numerical value of the elastic constant (23), which corresponds to the average potential (20),

$$k_{rr} = 1.56 \times 10^{17} k_\mathrm{B}T_\mathrm{tr} \text{ cm}^{-2}. \tag{28}$$

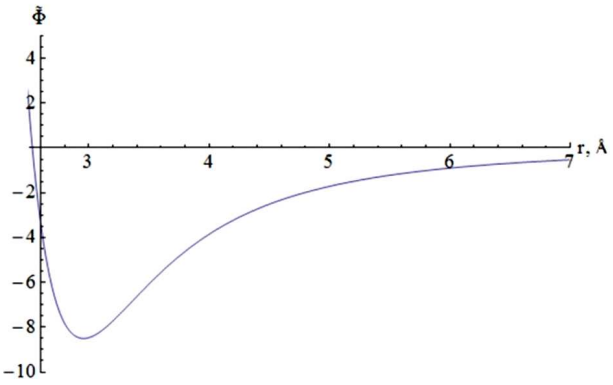

Fig. 11. Dependence of the interaction potential between water molecules in the dimer configuration on the distance between the oxygen atoms

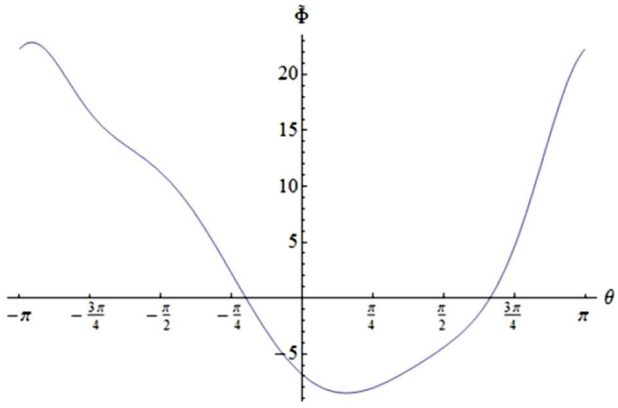

Fig. 12. Dependence of the dimer energy on the angle θ [18]

As one can see, the elastic constant corresponding to the average potential is three times smaller, i.e., this result agrees with qualitative considerations.

The longitudinal deviation of hydrogen from its equilibrium value at the triple point temperature equals

$$\frac{\left|\Delta r_{\mathrm{H}}^{(l)}\right|}{r_{\mathrm{d}}} \sim \frac{\sqrt{k_{\mathrm{B}}T_{\mathrm{tr}}/k_{rr}}}{r_{\mathrm{d}}} \approx 0.05. \tag{29}$$

6.1. Transverse vibrations of hydrogen bond

Transverse vibrations of the hydrogen bond are reduced to angular vibrations around the y- and z-axes. When analyzing these vibrations rigorously, one must also take into account the restrictions imposed by the immobility of the dimer's center of mass. However, we will consider only angular motions that satisfy the conditions of conservation of angular momentum projections onto the corresponding axes: $M_y = 0$ and $M_z = 0$.

6.1.1. Vibrations around y-axis

Let the angular deviations of the left and right molecules in the dimer (see Fig. 3) be described by the angles θ_1 and θ_2, respectively. The law of conservation of angular momentum yields the equation

$$I_{yy}^{(1)}\dot{\theta}_1 + I_{yy}^{(2)}\dot{\theta}_2 = 0, \tag{30}$$

where $I_{yy}^{(i)}$, $i = 1, 2$, are the moments of inertia of the left and right water molecules, respectively. From Fig. 3, we find

$$I_{yy}^{(1)} = 2m_{\mathrm{H}}r_{\mathrm{OH}}^2, \tag{31}$$

$$I_{yy}^{(2)} = 2m_{\mathrm{H}}r_{\mathrm{OH}}^2\cos^2\left(\frac{\alpha}{2}\right). \tag{32}$$

The hydrogen bond vibrations are directly related to the angle θ_1. From the above equations, it follows that

$$\dot{\theta}_1 = -\cos^2\left(\frac{\alpha}{2}\right)\dot{\theta}_2 \approx -\frac{3}{4}\dot{\theta}_2. \tag{33}$$

Since the variations of the angles θ_2 and θ_1 coincide, we obtain

$$\left\langle\theta_1^2\right\rangle \approx \frac{9k_{\mathrm{B}}T}{16k_{\theta\theta}}, \tag{34}$$

where the elastic constant k_{rr} is related to the angular dependence of the dimer energy in Fig. 12 by the standard relationship

$$k_{\theta\theta} = \left.\frac{\partial^2\Phi(r_{\mathrm{d}},\theta)}{\partial\theta^2}\right|_{\theta=\theta_{\mathrm{eq}}}. \tag{35}$$

Let us compare this value with that associated with the averaged potential. To an order of magnitude, the elastic longitudinal constant satisfies the equation

$$k_{rr}^{(a)} = \frac{1}{3}(k_{rr} + k_{\theta\theta} + k_{\varphi\varphi}). \tag{36}$$

Assuming that $k_{\varphi\varphi} \approx k_{\theta\theta}$, we obtain

$$k_{\theta\theta} \approx \frac{1}{2}(3k_{rr}^{(a)} - k_{rr}) \approx 0.23 \times 10^{17}k_{\mathrm{B}}T_{\mathrm{tr}}\ \mathrm{cm}^{-2}. \tag{37}$$

As one can see, the value of this elastic constant is approximately 20 times smaller than that corresponding

to longitudinal vibrations. Direct calculations of this elastic constant lead to an even smaller value,

$$k_{\theta\theta} \approx 0.15 \times 10^{17} k_{\rm B} T_{\rm tr} \ {\rm cm}^{-2}. \quad (38)$$

As a result, the amplitude of azimuthal vibrations increases by 4 to 5 times as compared to longitudinal vibrations. In other words, hydrogen-bond breaking becomes quite possible.

7. Discussion of Obtained Results

The clarification of the role of hydrogen bonds in the formation of water properties remains one of the issues that has not yet been fully resolved. This problem is analyzed in the presented article as well. Our approach is based on modeling hydrogen bonding in close connection with the structure of the water molecule, which takes into account the specific distribution of electron density generated by the oxygen. In particular, the appearance of hydrogen bonds in water is naturally associated with the formation of dimers. It was shown that the parameters of dimers in water, constructed on the basis of geometric considerations for individual water molecules, are in reasonably good agreement with experimental data. At the same time, it was found that transverse vibrations of hydrogen bonds are significantly less stable than their longitudinal components. As a result:

1) hydrogen bonds formed in water are short-term,

2) the magnitude of shear viscosity in water does not differ by an order of magnitude from that of argon and other low-molecular liquids.

Conditions for the formation of hydrogen bonds in water have been considered in detail, and it has been shown that they play a certain role throughout the entire liquid-state region, from the triple point to the critical point. The data obtained in this work are qualitatively consistent with those reported in works devoted to the dielectric permittivity and the heat capacity [7, 33]. Namely, our analysis supports the conclusions of those works, as well as the works on dipole relaxation [27–30], on the formation of molecular clusters; first of all, tetramers and dimers.

In this work, the physical nature of the characteristic temperature $T_{\rm H}$, which was established in Ref. [24] and plays an important role in determining the existence limits for living matter [25], has also been considered.

8. Conclusions

It was shown in this work that there are several important factors responsible for the emergence of short-term hydrogen bonds in liquid water. Among them, we note:

1) the geometric incompatibility of hydrogen bond formation with the density of water,

2) the instability of transverse vibrations of hydrogen bonds leading to dimerization and, in the more general case, to the clustering of water molecules.

The short-term existence of hydrogen bonds

1) forms the basis for the similarity of temperature dependences of the specific volume for water and argon, and

2) is responsible for the close values of viscosity in water and other low-molecular liquids.

In future research, we hope to expand and deepen the issues considered here; first of all, to develop the theory of the pH of pure water and aqueous salt solutions with dissolved carbon dioxide [34].

We sincerely thank the Academician of the NASU, Prof. Leonid Bulavin for formulating the problem and facilitating its comprehensive research. We would also like to note the great role of Prof. Volodymyr Gotsuls'kyi in the discussion of the results of this work during its implementation. The authors are pleased to thank Prof. Mykola Malomuzh for his help in preparing the article for publication.

1. D. Eisenberg, W. Kauzmann. *The Structure and Properties of Water* (Oxford University Press, 2005) [ISBN: 9780198570264].
2. M. Chaplin. *Water Structure and Science* (Retrieved, 2025).
3. S.G. Sotiriadou, K.D. Antoniadis, M.J. Assael, M.L. Huber. Reference correlation of the viscosity of argon. *Int. J. Thermophys.* **46**, 133 (2025).
4. O. Khorolskyi, N.P. Malomuzh. pH and H-bonding energy for pure water. *Chem. Phys. Lett.* **828**, 140713 (2023).
5. N.P. Malomuzh, O. Khorolskyi. Structure and properties of the hydroxonium ion. *Chem. Phys. Lett.* **858**, 141743 (2025).
6. H.J.C. Berendsen, J.P.M. Postma, W.F. van Gunsteren, J. Hermans. Interaction models for water in relation to protein hydration. In: *Intermolecular Forces*. Ed. by B. Pullman (D. Reidel Publishing Company, 1981) [ISBN: 9789027713261].
7. N.P. Malomuzh. Clustered structure of water and its argon-like equation of state. *RENSIT* **12** (1), 39 (2020).

8. R.A. Buckingham. The classical equation of state of gaseous helium, neon and argon. *Proc. R. Soc. Lond. A Math. Phys. Sci.* **168** (933), 264 (1938).
9. M. Rieth. *Nano-Engineering in Science and Technology: An Introduction to the World of Nano-design* (World Scientific Publishing Company, 2003) [ISBN: 9789812380746].
10. H.J.C. Berendsen, J.R. Grigera, T.P. Straatsma. The missing term in effective pair potentials. *J. Phys. Chem.* **91** (24), 6269 (1987).
11. W.L. Jorgensen, J. Chandrasekhar, J.D. Madura, R.W. Impey, M.L. Klein. Comparison of simple potential functions for simulating liquid water. *J. Chem. Phys.* **79**, 926 (1983).
12. W.L. Jorgensen. Transferable intermolecular potential functions for water, alcohols, and ethers. Application to liquid water. *J. Am. Chem. Soc.* **103**, 335 (1981).
13. J.A. Odutola, T.R. Dyke. Partially deuterated water dimers: Microwave spectra and structure. *J. Chem. Phys.* **72**, 5062 (1980).
14. U. Bergmann, A. Di Cicco, P. Wernet, E. Principi, P. Glatzel, A. Nilsson. Nearest-neighbor oxygen distances in liquid water and ice observed by x-ray Raman based extended x-ray absorption fine structure. *J. Chem. Phys.* **127**, 174504 (2007).
15. V.P. Voloshin, Y.I. Naberukhin. Hydrogen bond lifetime distributions in computer-simulated water. *J. Struct. Chem.* **50**, 78 (2009).
16. Y.I. Naberukhin, V.P. Voloshin. Distributions of hydrogen bond lifetimes in instantaneous and inherent structures of water. *Z. Phys. Chem.* **223**, 1119 (2009).
17. V.P. Voloshin, Yu.I. Naberukhin, G.G. Malenkov. Percolation analysis of the network of hydrogen water connections: the dyeing of connections on time of life and energy. *Struct. Dynam. Mol. Syst.* **10**, 12 (2011).
18. P.V. Makhlaychuk. The role of hydrogen bonds in the formation of water properties. Author's abstract of the dissertation of the candidate of physical and mathematical sciences: 01.04.02 (Odesa, 2013).
19. H.J.C. Berendsen, G.A. van der Velde. In: *CECAM Report of Workshop on Molecular Dynamics and Monte Carlo Calculations on Water*. Ed. by H.J.C. Berendsen (CECAM, 1972).
20. H. Umeyama, K. Morokuma. The origin of hydrogen bonding. An energy decomposition study. *J. Am. Chem. Soc.* **99** (5), 1316 (1977).
21. M. Schütz, S. Brdarski, P.-O. Widmark, R. Lindh, G. Karlström. The water dimer interaction energy: Convergence to the basis set limit at the correlated level. *J. Chem. Phys.* **107** (12), 4597 (1997).
22. W. Wagner, A. Pruss. The IAPWS formulation 1995 for the thermodynamic properties of ordinary water substance for general and scientific use. *J. Phys. Chem. Ref. Data* **31**, 387 (2002).
23. V.L. Kulinskii, N.P. Malomuzh. Dipole fluid as a basic model for the equation of state of ionic liquids in the vicitity of their critical point. *Phys. Rev. E* **67**, 011501 (2003).
24. L.A. Bulavin, N.P. Malomuzh. Upper temperature limit for the existence of the alive matter. *J. Mol. Liq. (Letter to the Editor)* **124**, 136 (2006).
25. A.I. Fisenko, N.P. Malomuzh. To what extent is water responsible for the maintenance of the life for warm-blooded organisms? *Int. J. Mol. Sci.* **10**, 2383 (2009).
26. A.A. Guslisty, O.D. Stoliaryk, O.V. Khorolskyi. Similarity between the electrophysical properties of albumin macromolecules and magnetic properties of paramagnets. *Ukr. J. Phys.* **70** (7), 460 (2025).
27. N.P. Malomuzh, V.N. Makhlaichuk, P.V. Makhlaichuk, K.N. Pankratov. Cluster structure of water in accordance with the data on dielectric permittivity and heat capacity. *J. Struct. Chem.* **54**, S205 (2013).
28. K. Okada, M. Yao, Y. Hiejima, H. Kohno, Y. Kajihara. Dielectric relaxation of water and heavy water in the whole fluid phase. *J. Chem. Phys.* **110**, 3026 (1999).
29. H.R. Pruppacher. Self-diffusion coefficient of supercooled water. *J. Chem. Phys.* **56**, 101 (1972).
30. J.H. Simpson, H.Y. Carr. Diffusion and nuclear spin relaxation in water. *Phys. Rev.* **111**, 1201 (1958).
31. A.I. Fisenko, N.P. Malomuzh, A.V. Oleynik. To what extent are thermodynamic properties of water argon-like? *Chem. Phys. Lett.* **450**, 297 (2008).
32. N.P. Malomuzh, K.S. Shakun. Collective components of self-diffusion in liquids. *Phys. Usp.* **64**, 157 (2021).
33. V.N. Makhlaichuk, N.P. Malomuzh. Manifestation of cluster excitations in dielectric properties of water vapor and liquid water as well as their heat capacity. *J. Mol. Liq.* **253**, 83 (2018).
34. O.D. Stoliaryk, O.V. Khorolskyi. Influence of atmospheric carbon dioxide on the acid-base balance in aqueous sodium chloride solutions. *Ukr. J. Phys.* **67** (7), 515 (2022).

Received 28.12.25.
Translated from Ukrainian by O.I. Voitenko

О.Д. Столярик, О.В. Хорольський

СПЕЦИФІКА ВОДНЕВИХ ЗВ'ЯЗКІВ У ВОДІ

У роботі аналізується специфіка прояву водневих зв'язків у структурних і термодинамічних властивостях води. Виходячи з певної структури молекули води, запропоновано новий механізм утворення димерів води й виникнення водневого зв'язку водночас. Встановлено, що характерні кути димеру води цілком задовільно узгоджуються з експериментальними даними. Показано, що взаємне відхилення кривих співіснування води й аргону зумовлено короткочасними водневими зв'язками в усьому інтервалі існування рідинного стану води. Доведено, що відсутність довготривалих водневих зв'язків у воді зумовлена нестабільністю їхніх поперечних теплових збуджень. Розглянуто характерні значення температури води у рідинному стані.

Ключові слова: вода, водневі зв'язки, термодинамічні властивості, кінетичні властивості.